British Journal of Pharmacology (2001) 134, 1195–1206 

www.nature.com/bjp

# Characterization of two *Bunodosoma granulifera* toxins active on cardiac sodium channels

[1]Cyril Goudet, [2]Tania Ferrer, [2]Loipa Galàn, [2]Adriana Artiles, [3]Cesar F.V. Batista, [3]Lourival D. Possani, [2]Julio Alvarez, [4]Abel Aneiros & *,[1]Jan Tytgat

[1]Laboratory of Toxicology, University of Leuven, E. Van Evenstraat 4, B-3000 Leuven, Belgium; [2]Instituto de Cardologia y Cirugia Cardiovascular, Apartado de Correos 6152, 10600 La Habana, Cuba; [3]Department of Molecular Recognition and Structural Biology, National Autonomous University of Mexico, Avenida Universidad, 2001 Apartado Postal 510-3, Cuernavaca 62210, Mexico and [4]Instituto de Oceanologia, Loma y 37 Alturas del Vedado, 10600 La Habana, Cuba

**1** Two sodium channel toxins, *Bg*II and *Bg*III, have been isolated and purified from the sea anemone *Bunodosoma granulifera*. Combining different techniques, we have investigated the electrophysiological properties of these toxins.

**2** We examined the effect of *Bg*II and *Bg*III on rat ventricular strips. These toxins prolong action potentials with $EC_{50}$ values of 60 and 660 nM and modify the resting potentials.

**3** The effect on $Na^+$ currents in rat cardiomyocytes was studied using the patch-clamp technique. *Bg*II and *Bg*III slow the rapid inactivation process and increase the current density with $EC_{50}$ values of 58 and 78 nM, respectively.

**4** On the cloned hH1 cardiac $Na^+$ channel expressed in *Xenopus laevis* oocytes, *Bg*II and *Bg*III slow the inactivation process of $Na^+$ currents (respective $EC_{50}$ values of 0.38 and 7.8 $\mu$M), shift the steady-state activation and inactivation parameters to more positive potentials and the reversal potential to more negative potentials.

**5** The amino acid sequences of these toxins are almost identical except for an asparagine at position 16 in *Bg*II which is replaced by an aspartic acid in *Bg*III. In all experiments, *Bg*II was more potent than *Bg*III suggesting that this conservative residue is important for the toxicity of sea anemone toxins.

**6** We conclude that *Bg*II and *Bg*III, generally known as neurotoxins, are also cardiotoxic and combine the classical effects of sea anemone $Na^+$ channels toxins (slowing of inactivation kinetics, shift of steady-state activation and inactivation parameters) with a striking decrease on the ionic selectivity of $Na^+$ channels.

*British Journal of Pharmacology* (2001) **134,** 1195–1206

**Keywords:** Sea anemone toxin; voltage-gated sodium channels; inactivation; ionic selectivity; cardiotoxin; neurotoxin

**Abbreviations:** ApA and ApB, *Anthopleura xanthogrammica* toxins A and B; ATX I and ATX II, *Anemonia sulcata* toxins I and II, *Bg*II and *Bg*III, *Bunodosoma granulifera* toxins II and III; HEPES, 2-[4-(2-hydroxyethyl)-1-piperazinyl] ethanesulphonic acid; Sh I, *Stychodactyla helianthus* toxin I; Tris, Tris(hydroxymethyl)aminomethane; TTX, Tetrodotoxin; VGSC, Voltage-Gated Sodium Channel

## Introduction

As key elements of signal transduction, voltage-gated sodium channels (VGSCs) are the target of toxins of various origins and chemical structures. The different effects of these toxins range from blocking the pore of the channel (e.g. tetrodotoxin, $\mu$-conotoxin) to modifying its gating and permeation characteristics (e.g. sea anemone toxins, scorpions $\alpha$- and $\beta$-toxins, batrachotoxin). These natural compounds are powerful tools for understanding the physiological contribution of VGSCs to cell and organ behaviour and for probing and correlating ion channel structure and function (Catterall, 1995; 2000; Cestele & Catterall, 2000; Denac *et al*., 2000; Lazdunski *et al*., 1986; Renaud *et al*., 1986). Moreover, elucidation of the mechanisms of action of toxins, knowledge of their 3D-structures and the discovery of common scaffolds between toxins open wide perspectives in designing various drugs (Ménez, 1998).

VGSCs are composed of a pore-forming $\alpha$ subunit of approximately 260 kDa flanked by two auxiliary $\beta$ subunits, a non covalently associated $\beta_1$ subunit of 36 kDa and a $\beta_2$ subunit of 33 kDa linked by a disulphide bond. In heterologous systems, expression of the $\alpha$ subunit alone is sufficient to form a functional $Na^+$ channel regulated by voltage. Membrane depolarization causes a voltage-dependent conformational change of the channel that induces an increase of its permeability to $Na^+$. This is followed by an inactivation process, wherein the channel closes and the permeability to $Na^+$ is shut off (Hille, 1992). The $\beta$ subunits, which do not form the pore, modulate the level of expression, channel gating properties, and interaction with cytoskeleton proteins (Catterall, 2000). Sodium channels can be differentiated by their primary structure, current kinetics and relative sensitivity to the neurotoxin tetrodotoxin (TTX). They have been cloned in

*Author for correspondence;
E-mail: Jan.Tytgat@farm.kuleuven.ac.be

different tissues of various species. The human cardiac isoform (hH1) of the VSGC (Gellens *et al*., 1992), or $Na_v$ 1.5 according to the recent nomenclature of VGSCs (Goldin *et al*., 2000), is a TTX-resistant channel expressed in cardiomyocytes where it plays a key role in the generation and propagation of the cardiac action potential (Balser, 1999).

Sea anemones produce several polypeptide toxins, mainly active on ionic channels of excitable membranes, to capture their prey. Sea anemone toxins acting on $Na^+$ channel have been intensively studied over the past years. They are both cardio- and neurotoxins and their main effects are to slow the inactivation process of $Na^+$ currents and to prolong the action potentials. These polypeptides cross-linked by three disulphide bridges and of molecular masses of approximately 5 kDa have been broadly categorized as type 1 (e.g. ATXI and ATXII from *Anemonia sulcata* (Wunderer & Eulitz, 1978; Wunderer *et al*., 1976), ApA and ApB from *Anthopleura xanthogrammica* (Norton, 1981; Reimer *et al*., 1985; Tanaka *et al*., 1977)) and type 2 (e.g. ShI from *Stichodactyla helianthus* (Kem *et al*., 1989; Wilcox *et al*., 1993)), according to amino acid sequence similarity and immunological cross-reactivity (Figure 2; see (Norton, 1991; Norton, 1998) for reviews). Toxins acting on $Na^+$ channels bind to at least six receptor sites (Catterall, 2000; Denac *et al*., 2000). Sea anemone toxins bind to receptor site 3, located in the extracellular linker between segments S3 and S4, in the fourth domain (D4). They share their receptor site with scorpion α-toxins (Gordon *et al*., 1998; Possani *et al*., 1999; Rogers *et al*., 1996) and funnel web spider toxins (Nicholson *et al*., 1994; 1998). The common point between these toxins is that they induce a slowing of the inactivation process of $Na^+$

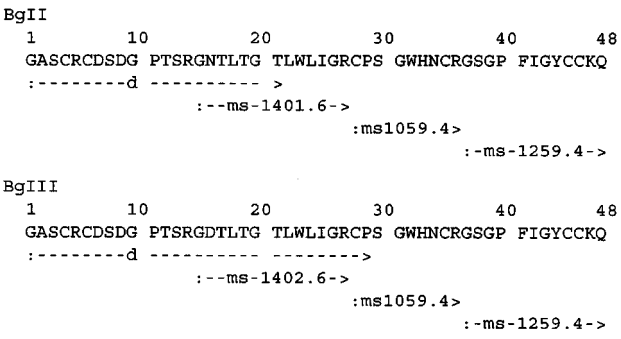


**Figure 1** Amino acid sequence determination of toxins. *Bg*II: Direct sequencing by Edman degradation of reduced and alkylated toxin provided unequivocal identification of the 21 first amino acids, shown by underlining (-d->). Three additional fragments were obtained by HPLC separation of toxin *Bg*II digested with Arg-C endopeptidase, which gave peptides with molecular masses of 1401.6, 1059.4 and 1259.4, respectively. The sequences were obtained by ionization, using MSIMS mass spectrometry, and correspond to sequence from positions 15 to 27, 28 to 36 and 37 to 48. The entire sequence corresponds exactly to that reported earlier (Loret *et al*., 1994). *Bg*III: Direct sequencing of reduced and alkylated toxin provided the 29 first amino acid residues, as indicated by the underlining (-d->). Three additional overlapping peptides were obtained by Arg-C endopeptidase digestion conducted as mentioned above for *Bg*II, in which the only difference was found in the peptide corresponding to positions 15 to 27 (molecular mass 1402.6) where an aspartic acid substitutes an asparagine in position 16. The MSIMS spectrometry analysis confirmed the sequences shown, which also corresponds exactly to those earlier reported (Loret *et al*., 1994). The numbers on top of the sequences indicate the positions of the amino acids in the sequences.

channels. From a mechanical point of view, the $Na^+$ channel inactivation process derives mainly from the voltage-dependent coupling of activation driven by the transmembrane movement of the voltage sensor (S4 segments). By binding to site 3, toxins prevent the normal gating movements of the IVS4 segment and thus uncouple $Na^+$ channel activation from inactivation (Catterall, 2000).

*Bunodosoma granulifera* is a common anemone of Cuban sea shores. Several active compounds with different pharmacological actions have been isolated from its secretions (Aneiros *et al*., 1993; Loret *et al*., 1994; Salinas *et al*., 1997). *Bg*II and *Bg*III are two toxins that have been purified and sequenced from this sea anemone originally by Loret *et al*. (1994). They consist in two peptides of 48 amino acids each containing six cysteine residues that form three disulphide bridges. The amino acid sequences of these two toxins possess a higher similarity with type 1 sea anemone toxins, like ApA and ApB or ATX II, than with the toxins of type 2, like ShI (Figure 2). The sequences of *Bg*II and *Bg*III are almost identical, only differing by a single amino acid. In *Bg*III, at position 16, an aspartic acid replaces the asparagine of *Bg*II (Figure 2). Despite their resemblance, the toxicity and the binding to rat brain synaptosomes of *Bg*II is interestingly significantly higher than that of *Bg*III. However, up to now, electrophysiological characterization of these two toxins was still completely lacking.

In the present study, combining different approaches, we have therefore investigated the electrophysiological properties of *Bg*II and *Bg*III toxins. Firstly, we have examined their effect on rat ventricular strips and observed that both toxins are able to prolong action potentials. Then, using the patch-clamp technique, we have studied the effect of *Bg*II and *Bg*III on $Na^+$ currents in cardiomyocytes revealing that these toxins slowed the rapid inactivation process of $Na^+$ currents and increased the current density. Finally, in order to refine our study, we have investigated the influence of these toxins on the cloned cardiac sodium channel hH1 expressed in *Xenopus laevis* oocytes, using the two-electrode voltage clamp technique. These experiments confirmed that *Bg*II and *Bg*III markedly slow the inactivation process of $Na^+$ currents in a dose-dependent way and showed that both steady-state inactivation and activation are shifted to more positive potentials. It was also revealed that toxin-modified channels displayed a decreased ionic selectivity. Moreover, effects of *Bg*II are more marked than effects of *Bg*III emphasizing the importance of the amino acid in position 16 for the biological effects of these two *Bunodosoma granulifera* toxins.

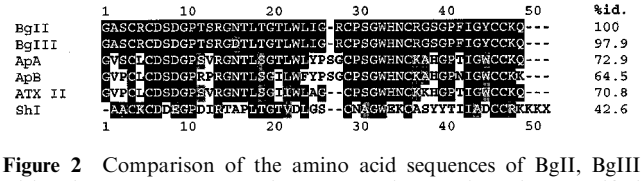


**Figure 2** Comparison of the amino acid sequences of BgII, BgIII with other sea anemone toxins. *Bg*II and *Bg*III have been purified from the sea anemone *Bunodosoma granulifera* (Loret *et al*., 1994), ATXII from *Anemonia sulcata* (Wunderer *et al*., 1976), ApA and ApB from *Anthopleura xanthogrammica* (Norton, 1981; Reimer *et al*., 1985; Tanaka *et al*., 1977) and ShI from *Stichodactyla helianthus* (Kem *et al*., 1989; Wilcox *et al*., 1993). Identical amino acids are indicated with a black background, homologous amino acids are indicated with a gray background and '%id' stands for the percentage of identity in comparison to *Bg*II. Dashes represent gaps.

## Methods

### *Toxin extraction and isolation*

Sea anemone *Bunodosoma granulifera* was collected along the north coast of Havana province, Cuba and transported to the laboratory in containers filled with sea water.

To prepare crude extract, in brief, 1 kg of *B. granulifera* was homogenized in 1 l of ethanol adjusted to pH 5.4 with acetic acid. After centrifugation (30 min, 4°C, $15{,}000 \times g$), the supernatant was separated and precipitated with 10 volumes of acetone (4°C, overnigth). The precipitate was recovered, diluted in water, concentrated under reduced pressure to eliminate acetone and freeze dried later. Lyophilized crude extract was dissolved in 0.10 M ammonium acetate pH 6.7 and gel filtered on Sephadex G-50 m ($4.5 \times 132$ cm) as previously described (Aneiros *et al*., 1993; Salinas *et al*., 1997).

The toxic peak was submitted to chromatography on the cation-exchanger Fractogel EMD $SO_3$-650 M ($1.2 \times 32$ cm) eluted with a linear gradient of ammonium acetate (pH 5.4) from 0.01 to 1.0 M. Toxins were rechromatographed on Fractogel EMD $SO_3$-650 M under analogous conditions, and desalted on Sephadex G-25. Further purification of toxins was performed by reversed-phase HPLC.

We used the toxicity test in crab to follow the toxic activity of chromatographic fractions during the purification procedures. The toxicity of the different fractions was evaluated as paralysing activity after injection on shore crabs (*Uca thayeri* and *Carcinus maenas*).

### *Mass spectrometry analysis*

The masses and sequences were obtained using a Finnigan LCQ-Duo ion trap mass spectrometer, equipped with an electrospray ion source. The analysis was performed as recently reviewed (Dongre *et al*., 1997).

### *Right ventricular strips*

Small right ventricular strips were dissected out from adult rat hearts fixed to a bath chamber and continuously superfused (10 ml $min^{-1}$) with normal Tyrode solution (NaCl, 140; KCl, 2.5; $CaCl_2$, 2; $MgCl_2$, 0.5; hydroxyethylpiperazine-N′-2-ethanesulfonic acid (HEPES), 10 and glucose, 5 (pH = 7.4, gassed with $O_2$)) at 35°C and field stimulated with 2 ms pulses at a frequency of 1.25 Hz (cycle length, 800 ms). Standard fine-tipped microelectrodes (tip resistance, 15 to 20 MΩ) were used to record action potentials (Alvarez *et al*., 1981). Action potential duration was measured at 0 ($D_0$) and −60 ($D_{-60}$) mV.

### *Isolation of adult ventricular cardiomyocytes*

Single rat ventricular cells were dispersed by a collagenase/trypsin enzymatic method similar to that previously described (Galan *et al*., 1998). In brief, rat hearts were cannulated through the aorta and perfused with a physiological solution for 5 min (in mM): NaCl 112.0, KCl 2.5, $CaCl_2$ 1.8, $MgCl_2$ 0.6, HEPES 10.0, glucose 5.0, $Na_2$-pyruvate 5.0, and pH adjusted to 7.4. Thereafter, the hearts were perfused with a low-$Ca^{2+}$ ($CaCl_2$ 30 μM) solution for 5 min. The hearts were then perfused for 30 min with the same solution containing collagenase (Boehringer Mannheim) and trypsin (Merck) at 1.5 mg $ml^{-1}$ and 0.4 mg $ml^{-1}$ respectively and supplemented with minimum essential medium (1 μl $ml^{-1}$ MEM; Sigma), creatine (5 mM) and taurine (20 mM). At the end of this period, the right ventricle was cut off and gently shaken in the same solution without enzymes. Isolated myocytes were kept in this physiological solution ($Ca^{2+} = 1$ mM) at room temperature (21–23°C) and used within 6–8 h.

### *Patch-clamp recordings*

The 'whole-cell' variant of the patch-clamp method was used (Hamill *et al*., 1981). Recordings were made using an RK-300 (Biologic, Claix, France) patch-clamp amplifier. Patch pipettes were made from borosilicate glass and had tip resistances between 1.0 and 1.2 MΩ. The pipette 'intracellular' solution contained (mM): CsCl 100, TEA-Cl 20, $MgCl_2$ 4.0, $Na_2$-GTP 0.5, $Na_2$-ATP 3, ethyleneglycol-bis-(-aminoethyl ether) N,N,N′,N′-tetraacetic acid (EGTA) 10, HEPES 10, the pH was adjusted to 7.2 with CsOH. For recording the $Na^+$ current ($I_{Na}$), $Ca^{2+}$ and $K^+$ currents were blocked by $CoCl_2$ (extracellular, 3 mM), tetraethylammonium chloride (TEA-Cl) and CsCl (intracellular and extracellular; see below), respectively. A cell aliquot was put in a Petri dish containing the control solution (mM): NaCl 112, KCl 2.5, $CaCl_2$ 1.8, $MgCl_2$ 0.6, HEPES 10, glucose 5.0, $Na_2$-pyruvate 5.0; pH was adjusted to 7.4 with NaOH. Experiments were performed at room temperature (22 ± 2°C).

After achieving the whole-cell patch-clamp configuration, each cell was exposed to different extracellular solutions by positioning it at the extremity of one of six capillaries (inner diameter of each capillary was 250 μm). Such a system allowed rapid changes of solution (<2 s). Currents were routinely evoked by 50 ms voltage-clamp pulses to −40 mV from a holding potential of −100 mV at a frequency of 0.25 Hz (cycle length 4 s). The current amplitude was estimated as the difference between the peak inward current and the current level at the end of a 50 ms pulse. The composition of the extracellular solution in these experiments was (in mM): NaCl 5, TEA-Cl 110, $CaCl_2$ 1.8, $MgCl_2$ 2, glucose 10, HEPES 10, pH was adjusted to 7.4 at 21°C. Pulse generation and data acquisition were done, using computer facilities and ACQUIS1 (CNRS License, France) software. Currents were filtered at 3 KHz and digitized at 20 KHz with a LabMaster DMA (model TM 125, Scientific Solutions, U.S.A.).

Current to voltage (I–V) relationships and availability curves were constructed using a standard double pulse voltage protocol. From a holding potential of −100 mV, a 50 ms test pulse to −40 mV was preceded by 50 ms prepulses to various membrane potentials. The time interval between pulses was 5 ms. I–V relationships were constructed from currents elicited by prepulse potentials. Normalization of current amplitudes at a given test pulse by the maximal current recorded as a function of prepulse potential gave the availability curve. The experimental points were fitted to a Boltzmann function:

$$I/I_{max} = (1 + \exp((V_p - V_{½})/s))^{-1} \quad (1)$$

where $V_p$ is the prepulse potential, $V_{1/2}$ is the potential for half-availability and s a slope factor.

The inactivation time course of currents was described by fitting the current traces between the inward peak and the end of the pulse using the fitting procedures of ACQUIS1 software. Recovery from inactivation was studied by a two pulse protocol. From a holding potential of −100 mV, a pair of 50 ms pulses to −40 mV was applied; the interval between the two pulses was varied from 5 to 650 ms. Recovery from inactivation (or reactivation) was obtained by the ratio of current measured at the second pulse to the current measured at the first pulse as a function of the time interval. Experimentally obtained means of the availability curves were fitted to a Boltzmann function to obtain the potential for half inactivation and slope factors.

Values are expressed as means ± s.e.means.

### *Expression in* Xenopus *oocytes*

For the expression in *Xenopus* oocytes, the hH1 gene was subcloned into pSP64T (Gellens *et al*., 1992). For *in vitro* transcription, hH1/pSP64T has been first linearized by *Xba*I. Then, capped cRNAs were synthetized from the linearized plasmid using the large-scale SP6 mMESSAGE-mMACHINE transcription kit (Ambion, U.S.A.). The *in vitro* synthesis of cRNA encoding hH1 and isolation of *Xenopus* oocytes was as previously described (Liman *et al*., 1992). Oocytes were injected with 50 nl of hH1 cRNA at a concentration of 1 ng $nl^{-1}$ using a Drummond microinjector (U.S.A.). The solution used for incubating the oocytes contained (in mM): NaCl 96, KCl 2, $CaCl_2$ 1.8, $MgCl_2$ 2 and HEPES 5 (pH 7.4), supplemented with 50 mg $l^{-1}$ gentamicin sulphate.

### *Electrophysiological recordings in* Xenopus *oocytes*

Whole-cell currents from oocytes were recorded from 1 to 3 days after injection using the two-electrode voltage clamp technique. Voltage and current electrodes were filled with 3 M KCl. Resistances of both electrodes were kept as low as possible (*ca*. 0.1 – 0.2 MΩ). During the experiments, the external NaCl concentration has been reduced in order to facilitate the clamp. Bath solution composition was (in mM): NaCl 40, KCl 2, $CaCl_2$ 1.8, $MgCl_2$ 2 and Tris-HCl 60 (pH 7.4). Experiments were performed using a GeneClamp 500 amplifier (Axon instruments, U.S.A.) controlled by a pClamp data acquisition system (Axon instruments, U.S.A.). Using a four-pole low-pass Bessel filter, currents were filtered at 5 kHz and sampled at 10 kHz. Digital leak subtraction of the current records was carried out using a P/4 protocol.

Current to voltage (I–V) relationships and steady-state activation curves were constructed using a standard single pulse voltage protocol. From a fixed holding potential of −90 mV, 25 ms test pulses to membrane potentials varying from −70 to +45 mV by 5 mV increments were performed. I–V relationships were constructed from peak currents elicited at different potentials. Normalization of conductance ($g/g_{max}$) as a function of the test pulse voltage gave the steady-state activation curve. The experimental points were fitted to a Boltzmann function:

$$g/g_{max} = (1 + \exp((V_p - V_{½act})/s))^{-1} \quad (2)$$

where $V_p$ is the pulse potential, $V_{1/2act}$ is the potential for half-activation and s a slope factor. Steady-state inactivation curves were constructed using a standard double pulse voltage protocol. From a fixed holding potential of −90 mV, a 50 ms test pulse to −20 mV was preceded by 50 ms prepulses to membrane potentials varying from −120 to 30 mV.

Normalization of the current amplitude at the test pulse by the maximal current recorded ($I/I_{max}$) as a function of prepulse potential gave the steady-state inactivation curve. The experimental points were fitted to a Boltzmann function:

$$I/I_{max} = (1 + \exp((V_p - V_{½inact})/s))^{-1} \quad (3)$$

where $V_p$ is the prepulse potential, $V_{1/2inact}$ is the potential for half-inactivation and s a slope factor. The permeability ratio of $Na^+$ as compared to $K^+$ ($P_{Na}/P_K$) has been calculated using the Goldman-Hodgkin-Katz (GHK) equation:

$$E_{rev} = (RT/zF)\ \mathrm{In}\ ((P_{Na}[Na]_o + P_K[K]_o)/(P_{Na}[Na]_i + P_K[K]_i)) \quad (4)$$

where $E_{rev}$ is the reversal potential determined from the I–V relationship, $P_{Na}$ and $P_K$ are the permeabilities of the channel for $Na^+$ and $K^+$, respectively. The external concentrations of $Na^+$, $[Na]_o$, and $K^+$, $[K]_o$, were 40 and 2 mM, respectively. The internal concentrations of $Na^+$, $[Na]_i$, and $K^+$, $[K]_i$, have been estimated to be 6 and 92 mM, respectively (Dascal, 1987).

The inactivation time course of $Na^+$ currents was described by fitting the current traces between the inward peak and the end of the pulse using the fitting procedures of pClamp6 software (Axon instruments, U.S.A.).

Data are presented as mean ± s.e.mean. All experiments were performed at room temperature (20 ± 2°C).

## Results

### *Toxin identification*

After gel filtration chromatography on Sephadex G-50, only fraction three eluting between 70 – 80% of one whole column volume was found to be toxic in the crab bioassay. This fraction was submitted to a cation exchange chromatography on Fractogel EMD $SO_3$-650M. The fractions eluting in the gradient at ammonium acetate concentrations between 0.1 and 0.2 M were further chromatographed under the same conditions to give the toxins (*Bg*III and *Bg*II respectively) that were earlier reported by Loret *et al*. (1994).

For *Bg*II toxin, a direct sequencing by Edman degradation of reduced and alkylated toxin provided an unequivocal identification of the 21 first amino acids. Then, following a digestion of this toxin with Arg-C endopeptidase a HPLC separation gave three additional fragments with molecular masses of 1401.6, 1059.4 and 1259.4, respectively. The sequences were obtained by ionization, using MS/MS mass spectrometry, and correspond to sequences from position 15 to 27, 28 to 36 and 37 to 48. The entire sequence corresponds exactly to that earlier reported by Loret *et al*., 1994 (Figure 1).

For *Bg*III toxin, a direct sequencing by Edman degradation of reduced and alkylated toxin provided an unequivocal identification of the 29 first amino acids. Then, overlapping

peptides were obtained by Arg-C endopeptidase digestion conducted as mentioned above for *Bg*II, in which the only difference was found in the peptide corresponding to positions 15 to 27 (molecular mass 1402.6) where an aspartic acid substitutes an asparagine in position 16. The MS/MS spectrometry analysis confirmed the sequences shown, which also corresponds exactly to those earlier reported by Loret *et al*., 1994 (Figure 1).

*Bg*II and *Bg*III consist in two peptides of 48 amino acids which each contain six cysteine residues forming three disulphide bridges. The measured masses for *Bg*II and *Bg*III, 5072.7 Da and 5073.1 Da, respectively, are almost identical to the theoretical masses determined according to the amino acid sequences, 5071.7 Da and 5072.7 Da for *Bg*II and *Bg*III, respectively. In Figure 2, amino acid sequences of *Bg*II and *Bg*III are shown and compared with other sea anemone $Na^+$ channel toxins: ATXII from *Anemonia sulcata* (Wunderer *et al*., 1976), ApA and ApB from *Anthopleura xanthogrammica* (Norton, 1981; Reimer *et al*., 1985; Tanaka *et al*., 1977) and *Sh*I from *Stichodactyla helianthus* (Kem *et al*., 1989; Wilcox *et al*., 1993). The amino acid sequence of *Bg*ll possesses a higher similarity with type 1 sea anemone toxins (72.9%, 64.5% and 70.8% identity with ApA, ApB and ATX II, respectively) than with the toxins of type 2 (42.6% identity with *Sh*I).

### *Effects of* Bunodosoma granulifera *toxins on action potentials of rat ventricular strip*

Superfusion of rat ventricular strips with 10 $\mu$M *Bg*II or *Bg*III toxins induced a fast increase in action potential duration (Figure 3). Within 1 min, action potential duration at 0 mV ($D_0$) was increased to 160 and 130% of control in the presence of *Bg*II and *Bg*III, respectively. Action potential duration at $-60$ mV ($D_{-60}$) was increased to 230 and 185% in the presence of *Bg*II and *Bg*III, respectively. During this initial period, no major changes were observed in action potential amplitude or resting membrane potential. At longer superfusion times (5 min), action potential duration was further increased and the resting potential decreased. Interestingly, these changes were more marked with *Bg*II which increased $D_0$ to 560% of control and decreased resting potential from $-92$ to $-45$ mV. Under the action of *Bg*III, $D_0$ was only further increased to 216% of control while the resting potential was decreased from $-93$ to $-87$ mV.

The increase of the action potential duration induced by *Bg*II and *Bg*III is dose-dependent. The effect of *Bg*II and *Bg*III has been studied at concentrations ranging from 0.01 to 10 $\mu$M and revealed that *Bg*II is more potent than *Bg*III. The toxin concentration producing the half maximum effect ($EC_{50}$) on the action potential duration at 0 mV determined by a sigmoidal fit is $60\pm4$ nM for *Bg*II ($n=3$) and $663\pm380$ nM for *Bg*III ($n=3$).

### *Effects of* Bg*II and* Bg*III on $Na^+$ current of rat ventricular cardiomyocytes*

To study the effect of *Bunodosoma granulifera* toxins on the $Na^+$ current ($I_{Na}$), rat ventricular myocytes were superfused with an extracellular solution containing 5 mM NaCl so as to decrease $I_{Na}$ amplitude and to obtain a better voltage-clamp control. Myocytes were held at $-100$ mV and routinely depolarized to $-40$ mV with 50 ms voltage-clamp pulses to monitor $I_{Na}$. Membrane capacity was determined in voltage-clamped cells (Galan *et al*., 1998) and the mean value obtained from 27 cells was $124.5\pm18.3$ pF. Ionic current amplitudes were normalized to membrane capacity and are expressed as current density (pA/pF). Under these experi-

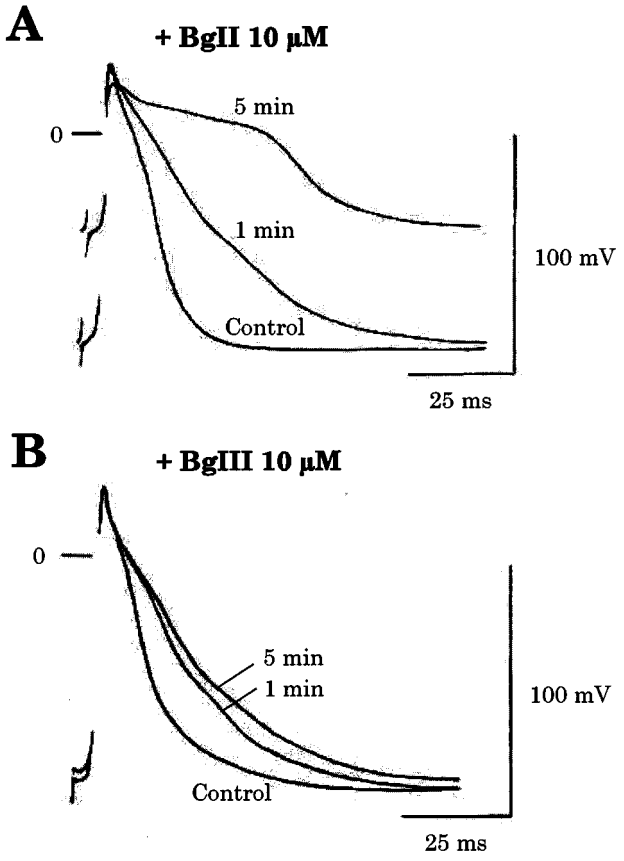


**Figure 3** Effects of *Bunodosoma granulifera* toxins on the resting and action potential characteristics of rat ventricular strips. Both *Bg*II (A) and BgIII (B) were applied at a concentration of 10 $\mu$M. Within 1 min, both toxins markedly increased the action potential duration. After a longer time (5 min) the resting potential was decreased. Note that the increase in action potential duration and the decrease in resting potential were more marked with *Bg*II.

**Table 1** Effects of *Bg*II and *Bg*III on $I_{Na}$ of rat ventricular cardiomyocytes (values are expressed as per cent increase over control value)

| Bg*II molar concentration* | $10^{-9}$ | $10^{-8}$ | $10^{-7}$ | $10^{-6}$ | $10^{-5}$ |
|---|---|---|---|---|---|
| $I_{Na}$ density | 0 | $15\pm10$ | $100\pm8$* | $152\pm17$* | $144\pm12$* |
| $T_{50\%}$ | 0 | $10\pm8$ | $273\pm5$* | $246\pm6$* | $301\pm10$* |
| Number of cells | 5 | 5 | 6 | 7 | 6 |
| Bg*III molar concentration* | $10^{-9}$ | $10^{-8}$ | $10^{-7}$ | $10^{-6}$ | $10^{-5}$ |
| $I_{Na}$ density | 0 | $9\pm8$ | $92\pm9$* | $167\pm15$* | $127\pm10$* |
| $T_{50\%}$ | 0 | $22\pm9$ | $261\pm12$* | $234\pm10$* | $281\pm12$* |
| Number of cells | 4 | 5 | 5 | 6 | 5 |

*$P<0.05$ respect to control; $T_{50\%}$: time for half inactivation of $I_{Na}$ ($I_{Na}$ was evoked at $-40$ mV from a holding potential of $-100$ mV)

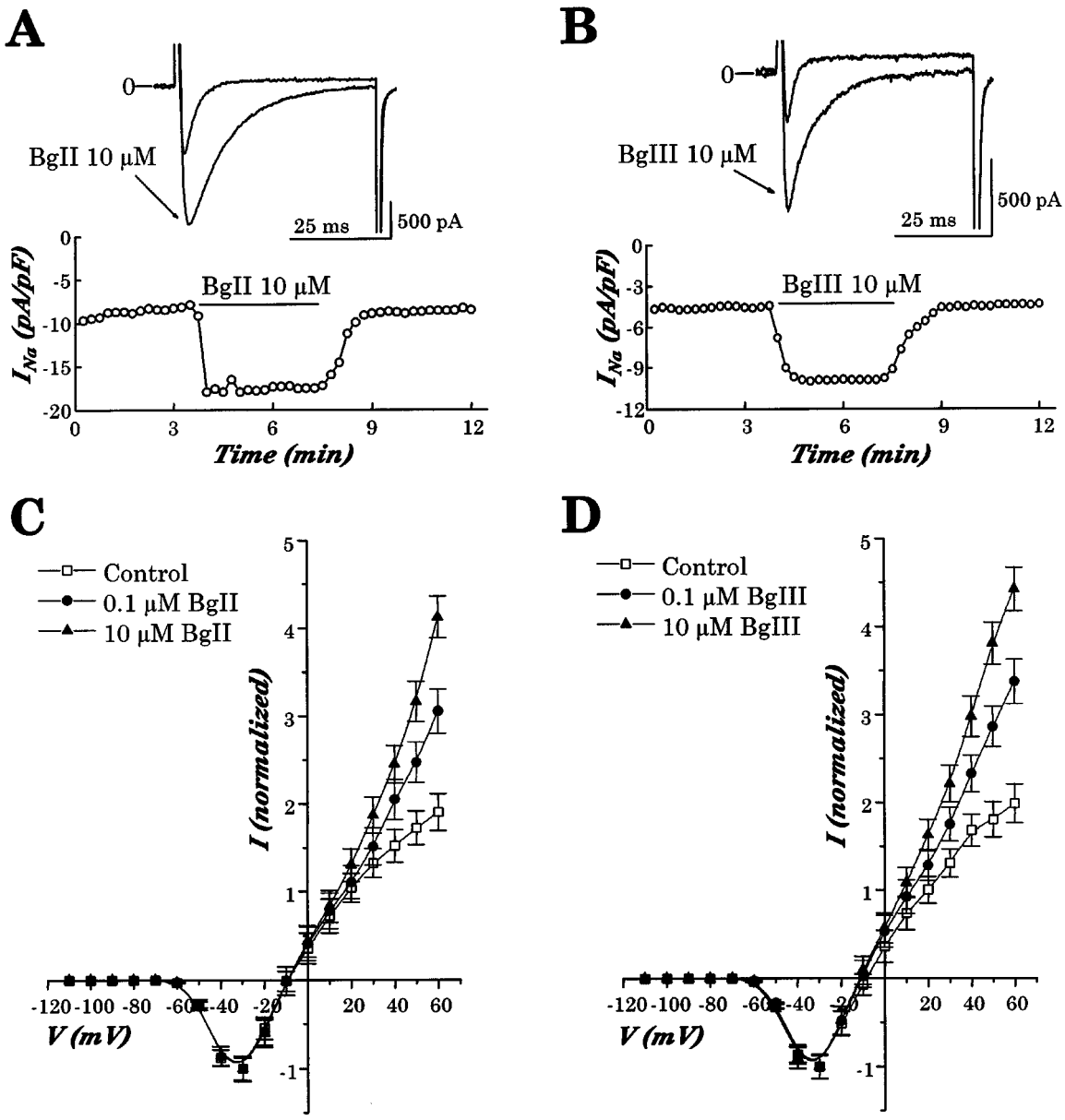


**Figure 4** Effect of *Bg*II and *Bg*III toxins on $Na^+$ currents in rat ventricular cardiomyocytes. (A,B) Time course of the effects of 10 $\mu$M *Bg*II or 10 $\mu$M *Bg*III on $I_{Na}$ of a rat ventricular cardiomyocyte. Points represent $I_{Na}$ density values (pA/pF) at $-40$ mV. The holding potential was $-100$ mV. The thick horizontal line indicates the period during which the cell was superfused with the toxin. The inset on the top shows current traces recorded in control condition and during the action of toxins. Note in these cells, the marked increase in current amplitude and the slowing of inactivation. (C,D) Averaged normalized current-voltage relationship of $I_{Na}$ established in six cells under control conditions and in the presence of 0.1 and 10 $\mu$M *Bg*II (A) or 0.1 10 $\mu$M *Bg*III (B).

mental conditions $I_{Na}$ at $-40$ mV had a density of $-7.4\pm0.9$ pA/pF ($n=27$).

Both *Bg*II and *Bg*III exerted concentration-dependent effects on the $I_{Na}$ amplitude and the inactivation time course. At low concentrations ($10^{-9}$, $10^{-8}$ M), no significant effects were seen. At higher concentrations ($10^{-7}$ to $10^{-5}$ M), both toxins increased the peak $I_{Na}$ density at $-40$ mV and delayed its inactivation time course. Table 1 summarizes the obtained results.

In the present experimental conditions (i.e. 5 mM external $Na^+$ concentration), the inactivation time course of $I_{Na}$ could be described by a double exponential function in about 50% of the cells. In the other half, a best fit was obtained by a single exponential function. In addition, in most cells, the inactivation time course in the presence of toxin was best described by a single exponential. For these reasons, we chose to measure the half inactivation time of $I_{Na}$ ($T_{50\%}$) as an indication of the slowing of the inactivation time course induced by *Bg*II and *Bg*III (Table 1).

The effects of both *Bg*II and *Bg*III on $I_{Na}$ were rapidly achieved (Figure 4A, B). Steady-state effects were commonly reached in 10–15 s and were stable throughout the 4–5 min period of exposure to the toxins. Washout of toxin effect was complete for both *Bg*II and *Bg*III and took approximately 30 s (Figure 4A,B). The $EC_{50}$ of the toxins on $I_{Na}$

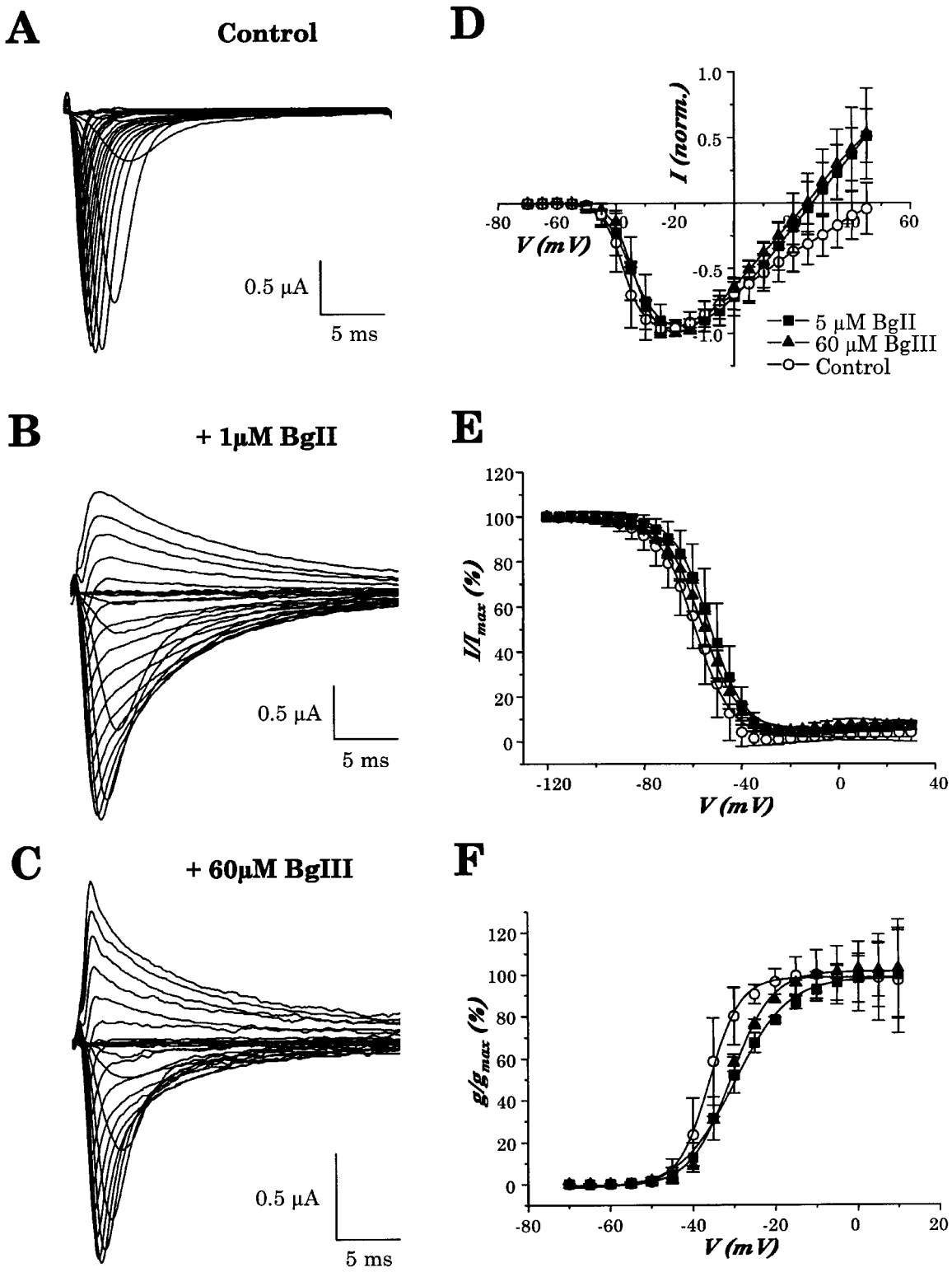


**Figure 5** Effect of *Bg*II and *Bg*III toxins on the cloned hH1 channel expressed in *Xenopus* oocytes. (A–C) Representative family of current traces evoked in an oocyte expressing hH1 channel by depolarizations ranging between −70 to +45 mV, using 5 mV increments, from a holding potential of −90 mV, in control conditions (A), in the presence of 1 μM *Bg*II toxin (B) and in the presence of 60 μM *Bg*III toxin (C). Note that the slowing of inactivation is more marked with *Bg*II than with *Bg*III and also the emergence of outward currents in the presence of both toxins. (D) Averaged normalized current-voltage relationship of hH1 in control conditions, in the presence of 5 μM of *Bg*II toxin or 60 μM of *Bg*III toxin. (E) Averaged normalized steady-state inactivation in control condition, in the presence of 5 μM of *Bg*II toxin or 60 μM of *Bg*III toxin. (F) Average normalized steady-state activation in the absence of toxins, in the presence of 5 μM of *Bg*II toxin or 60 μM of *Bg*III toxin. In (D–F), data are mean±s.e.mean of $n=20$, $n=6$ and $n=4$ experiments, respectively.

determined by a sigmoidal fit is $58\pm8$ nM for *Bg*II ($n=5$) and $78\pm48$ nM for *Bg*III ($n=5$). Moreover, these actions of *Bg*II and *Bg*III on $I_{Na}$ were voltage-dependent, the effects being more marked at positive potentials. Normalized current to voltage relationships were established under control condition and after superfusion of the myocytes with 0.1 and 10 $\mu$M *Bg*II or *Bg*III (Figure 4C,D). Under non-normalized conditions, 10 $\mu$M *Bg*II and *Bg*III increased $I_{Na}$ at $-40$ mV to $144.3\pm12.0\%$ and $127.4\pm10.2\%$, of controls, respectively. At $+60$ mV, the large outward $I_{Na}$ was increased to $306.2\pm15.2\%$ and $304.6\pm16.5\%$ of controls, respectively.

The actions of *Bg*II and *Bg*III on $I_{Na}$ were further characterized at a concentration of 10 $\mu$M by establishing availability and recovery from inactivation (reactivation) curves (see Methods). Under control condition, best fittings of the experimental means to a Boltzmann function gave a half inactivation potential and slope factor of $-80\pm2$ mV and $6.6\pm0.3$ mV, respectively. After application of 10 $\mu$M *Bg*II ($n=6$) and *Bg*III ($n=5$) they were $-83\pm3$ mV and $7.8\pm0.4$ mV and $-77\pm3$ mV and $6.2\pm0.4$ mV, respectively. Except for the change in the slope factor in the presence of *Bg*II ($P<0.05$), these values were not significantly different from the ones measured in control. However, it should be emphasized that both *Bg*II or *Bg*III increased $I_{Na}$ availability at potentials between $-60$ and $-40$ mV with respect to control. For example, at $-40$ mV availability increased from 0 to $0.13\pm0.01$ and to $0.10\pm0.01$ with *Bg*II and *Bg*III respectively (data not shown).

Recovery from inactivation (reactivation) was established in control condition and after superfusion of the cells with 10 $\mu$M *Bg*II and *Bg*III. In control condition, the time to reach the half reactivation level of $I_{Na}$ was $35.2\pm6.0$ ms. Neither *Bg*II ($n=4$) nor *Bg*III ($n=4$) exerted significant effects on $I_{Na}$ recovery from inactivation; times for half reactivation were $32.5\pm5.3$ ms and $31.8\pm7.3$ ms, respectively.

### *Effect of* Bg*II and* Bg*III toxins on cloned hH1 $Na^+$ channel expressed in* Xenopus *oocytes*

Families of $Na^+$ current recorded using the two-electrode voltage-clamp technique on *Xenopus* oocytes expressing hH1 channels are shown in Figure 5. Currents traces were evoked by step depolarizations of 25 ms ranging from $-70$ to $+45$ mV, using intervals of 5 mV, from a holding potential of $-90$ mV. While in control conditions (Figure 5A), $Na^+$ currents inactivated rapidly, the inactivation kinetics strongly slowed down at the different voltages in the presence of 1 $\mu$M *Bg*II (Figure 5B) or 60 $\mu$M *Bg*III (Figure 5C) toxin. The slowing of the inactivation process induced by 1 $\mu$M of *Bg*II was stronger than the one induced by 60 $\mu$M of *Bg*III. While almost all the channels closed after 25 ms in control conditions, a bigger proportion of channels remained open and led to a persistent current in the presence of the toxins. Another interesting observation is that, although in control conditions only inward $Na^+$ currents can be seen in the voltage range of $-70$ to $+45$ mV, clear outward $Na^+$ currents appeared at the most positive voltages, in the presence of 1 $\mu$M *Bg*II or 60 $\mu$M *Bg*III toxin.

Current to voltage (I-V) relationships are displayed in the Figure 5D, in the absence and presence of 5 $\mu$M and 60 $\mu$M of *Bg*II and *Bg*III, respectively. The I-V curves reveal that *Bg*II and *Bg*III induced a depolarizing shift in the threshold of activation of the hH1 channel. This shift is confirmed by the voltage dependence of steady-state activation shown in Figure 5F. In control conditions, the half activation voltage ($V_{1/2act}$) and the slope factor measured by a Boltzmann fit of the activation curve are $-37.0\pm0.2$ mV and $3.8\pm0.2$ mV ($n=20$), respectively. In the presence of 5 $\mu$M *Bg*II, $V_{1/2act}$ is $-30.0\pm0.4$ mV and the slope factor is $6.5\pm0.4$ mV ($n=6$). In the presence of 60 $\mu$M *Bg*III, $V_{1/2act}$ is $-30.8\pm0.3$ mV and the slope factor is $5.0\pm0.3$ mV ($n=4$). Thus, *Bg*II and *Bg*III induce a relatively similar shift of $+7.0$ mV and $+6.2$ mV of the $V_{1/2act}$ values, respectively but *Bg*II is more potent than *Bg*III. Moreover, as can be anticipated from the emergence of outward currents upon toxin application in Figure 5A–C, the reversal potential ($E_{rev}$) changes in the presence of toxins (Figure 5D). In control conditions, $E_{rev}$ is $44.4\pm7.4$ mV ($n=20$) while $E_{rev}$ measured in the presence of 5 $\mu$M *Bg*II and 60 $\mu$M *Bg*III is $26.3\pm6.4$ mV ($n=6$) and $27.0\pm7.4$ mV ($n=4$), respectively. This will be further discussed below.

Figure 5E shows the voltage dependence of steady-state sodium channel inactivation in the absence and presence of 5 and 60 $\mu$M of *Bg*II and *Bg*III, respectively. Measurements of steady-state inactivation were made following a standard two-pulse protocol. A 50 ms conditioning pulse ranging from $-120$ to 30 mV was followed by a 50 ms test pulse at $-20$ mV. In control conditions, a prepulse of $-120$ mV forces all the channels in the resting state and make these fully available for activation during the test pulse. In contrast to this, a prepulse of $-30$ mV moves all the channels in the inactivated state and thus non-available for activation during the test pulse. The voltage at which half of the channels are inactivated ($V_{1/2inact}$) and the slope factor determined by a Boltzmann fit of the inactivation curve are $-58.9\pm0.4$ and $7.4\pm0.3$ mV, respectively. *Bg*II and *Bg*III induce a depolarizing shift in the steady-state inactivation of the hH1 channel. In the presence of 5 $\mu$M *Bg*II, $V_{1/2inact}$ and the slope factor are $-53.2\pm0.3$ mV and $7.1\pm0.2$ mV ($n=6$), respectively. In the presence of 60 $\mu$M *Bg*III, $V_{1/2inact}$ and the slope factor are $-56.1\pm0.3$ mV and $7.3\pm0.3$ mV ($n=4$), respectively. Thus, saturating concentrations of *Bg*II and *Bg*III cause a shift of $+5.7$ mV and $+3.8$ mV, respectively, in the voltage at which half the hH1 $Na^+$ channels are inactivated.

The inactivation time course of hH1 increased with the concentration of toxin (Figure 6). Figure 6A,B display the effect of different concentrations of *Bg*II and *Bg*III on $Na^+$ currents carried by hH1 and evoked by a step depolarization to 0 mV for 25 ms from a holding potential of $-90$ mV. As can be seen on these different current traces, the slowing of the inactivation induced by *Bg*II and *Bg*III is clearly concentration-dependent, with an effect more pronounced for *Bg*II than *Bg*III. The inactivation process can be fitted satisfactorily by a single exponential. The relationship between *Bg*II and *Bg*III concentration and the obtained $\tau$-values are displayed in Figure 6C,D, respectively. It can be seen that $\tau$ increased as a function of the concentration of the toxins. In control condition, $\tau$ was $1.0\pm0.1$ ms ($n=17$). In the presence of 1 $\mu$M *Bg*II or 100 $\mu$M *Bg*III, $\tau$ increased to $5.8\pm0.6$ ($n=5$) and $4.6\pm0.4$ ms ($n=3$), respectively. The increase of $\tau$ is thus approximately 25% more important in the presence of *Bg*II than in the presence of *Bg*III. The concentration of the toxin producing the half maximum effect

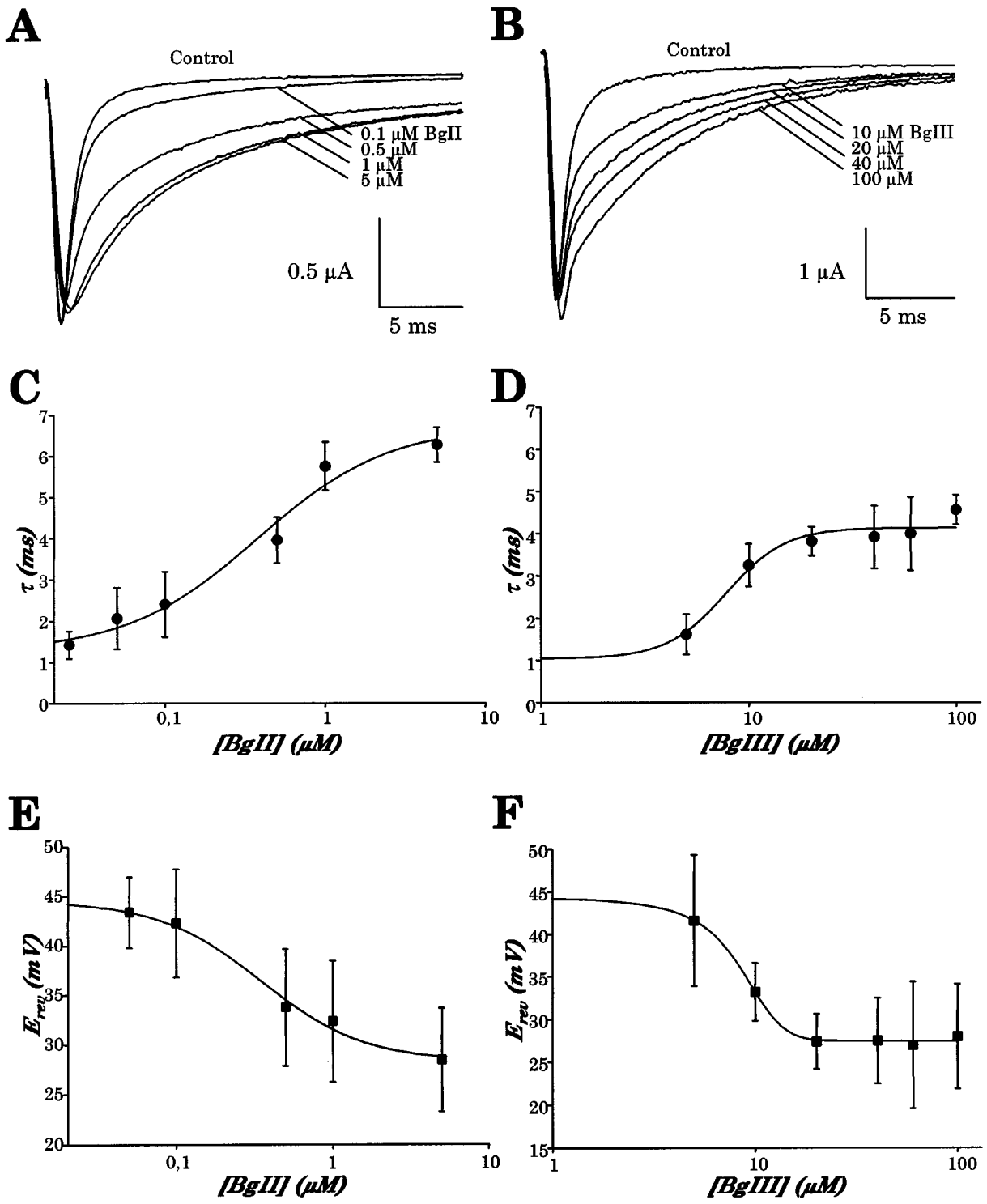


**Figure 6** Concentration dependence of the slowing of inactivation and of the modification of the reversal potential induced by *Bg*II and *Bg*III toxins on hH1 $Na^+$ channels. (A) Current traces were evoked by a step depolarization to 0 mV lasting 25 ms from a holding potential of −90 mV, in the absence (control) and in the presence of increasing concentrations of *Bg*II toxin (as indicated), using the same oocyte. (B) Same protocol as in (A) but in the absence (control) and in the presence of increasing concentrations of *Bg*III toxin (as indicated), in the same oocyte. (C) Averaged time constant of inactivation ($\tau$) plotted *vs* concentration of *Bg*II toxin. Time constants of inactivation were calculated from a first order exponential fit of current traces evoked by a step depolarization to 0 mV from a holding potential of −90 mV. The $EC_{50}$ value determined by a sigmoidal fit is 382±140 nM. Data are the mean±s.e.mean of at least three experiments. (D) Averaged time constant inactivation ($\tau$) plotted *vs* concentration of *Bg*III toxin. Time constants of inactivation were calculated as in (C). The $EC_{50}$ value as determined by a sigmoidal fit of $\tau$ is 7.8±1.2 μM. (E) Averaged reversal potential plotted *vs* concentration of *Bg*II toxin. The $EC_{50}$ value determined by a sigmoidal fit is 340±70 nM. (F) Averaged reversal potential plotted *vs* concentration of *Bg*III toxin. The $EC_{50}$ value determined by a sigmoidal fit is 8.4±0.3 μM. Data are the mean±s.e.mean of at least three experiments at each concentration.

on the inactivation time constant ($EC_{50}$) determined by a sigmoidal fit is $382 \pm 140$ nM for *Bg*II and $7.8 \pm 1.2$ $\mu$M for *Bg*III. From this follows that *Bg*II is approximately 20 times more potent than *Bg*III.

As can be seen in the current-voltage relationships in Figure 5D, *Bg*II and *Bg*III induce a shift of the reversal potential. In control conditions, the reversal potential of $Na^+$ currents generated by hH1 channels is $44.4 \pm 7.4$ mV ($n=20$). In the presence of 5 $\mu$M *Bg*II and 100 $\mu$M *Bg*III, $E_{rev}$ is $28.5 \pm 5.2$ mV and $28.0 \pm 6.1$ mV, respectively ($n=4$ and 3). The maximal shifts of $E_{rev}$ as induced by *Bg*II and *Bg*III are very similar, $-15.9$ and $-16.4$ mV, respectively. A statistical analysis shows that the differences of $E_{rev}$ in the absence or in the presence of toxins are significant (Student's *t*-test, $P<0.05$). The permeability ratio of $Na^+$ over $K^+$ ($P_{Na}/P_K$) determined from the measured $E_{rev}$ using the GHK equation (see Methods) decreases from 84 in control condition to 12.3 and 12.7 in the presence of 5 $\mu$M *Bg*II and 100 $\mu$M *Bg*III, respectively. This represents a 6.8 and 6.6 fold decrease in the ionic selectivity for $Na^+$ over $K^+$ of the hH1 channel in the presence of the toxins. Similarly, the modification of the reversal potential induced by *Bg*II and *Bg*III observed in a different external concentration of $Na^+$ (96 mM) resulted in a 7 and 6.7 fold decrease in the ionic selectivity for $Na^+$ over $K^+$ in the presence of 5 $\mu$M *Bg*II and 100 $\mu$M *Bg*III, respectively (data not shown). In the same experimental conditions (40 mM external $Na^+$), the reversal potential of hH1 is not modified in the presence of 1 $\mu$M ATX II (data not shown).

Figure 6E,F display the concentration dependence of the reversal potential of hH1 channels as a function of the concentration of *Bg*II or *Bg*III toxins. The $EC_{50}$ determined by a sigmoidal fit is $340 \pm 70$ nM for *Bg*II and $8.4 \pm 0.3$ $\mu$M for *Bg*III. These $EC_{50}$ values are very comparable with the ones obtained by fitting the toxin concentration dependence of the time constant of inactivation. In both cases, i.e. $E_{rev}$ and time constant of inactivation measurements, it is clear that *Bg*II is more potent than *Bg*III.

## Discussion

In rat ventricular strips, *Bg*II and *Bg*III significantly prolong the action potentials and induce a decrease of the resting potential in a concentration-dependent way. The half maximum effect ($EC_{50}$) on the action potential duration at 0 mV is 60 nM for *Bg*II and 663 nM for *Bg*III. In rat cardiac myocytes, patch-clamp studies point out that *Bg*II and *Bg*III, at concentrations ranging from 0.1 to 10 $\mu$M, increased $Na^+$ current density (with an effect more pronounced at positive voltages) and delayed its inactivation time course (Figure 4). The electrophysiological effect of *Bg*II and *Bg*III relates to the mechanisms of action of other $Na^+$ channels toxins from sea anemone, for example the well known ATX II from *Anemonia sulcata* (Alsen *et al*., 1981; Chahine *et al*., 1996; Ravens, 1976; Ulbricht & Schmidtmayer, 1981), ApA and ApB from *Anthopleura xanthogrammica* (Benzinger *et al*., 1997; Kudo & Shibata, 1980; Shibata *et al*., 1976), or the recently isolated APE 1.1, APE 1.2, APE 2.1, APE 2.2 and APE 5.3 from *Anthopleura elegentissima* (Bruhn *et al*., 2001). Similarly to *Bg*II and *Bg*III, these toxins inhibit the inactivation process of $Na^+$ channels which leads to cardiotoxic (arrhythmia) and neurotoxic (repetitive firing) effects. In comparison, the $EC_{50}$ values of the $Na^+$ influx increase induced by ApA, ApB and ATXII in rat cardiac tissues are 3, 2 and 15 nM, respectively (Schweitz *et al*., 1981).

Although in this study, we focused on the cardiotoxicity of these toxins, Loret *et al*. (1994) have shown in their experiments that *Bg*II and *Bg*III are also potent neurotoxins. When injected intracerebroventricularly to mice, *Bg*II and *Bg*III present $LD_{50}$ values of 0.4 and 21 $\mu g\ kg^{-1}$, respectively. Moreover, binding competition assays of these toxins with Aahll, a scorpion toxin also acting on site 3 of $Na^+$ channels, resulted in a $K_d$ of 9 nM for *Bg*II and 72 nM for *Bg*III. Likewise, recent patch-clamp experiments in cultured neurons have shown that *Bg*II is able to interact with neuronal $Na^+$ channels (E. Salceda, personal communication).

In order to deepen our comprehension on the molecular mechanisms of action of *Bg*II and *Bg*III toxins, we performed voltage-clamp studies of the cloned cardiac $Na^+$ channel hH1 expressed in *Xenopus* oocytes. Our experiments show that the main effect induced by *Bg*II and *Bg*III is a marked and concentration-dependent slowing of the inactivation process of $Na^+$ current associated with a decrease of the ionic selectivity of the channel. Interestingly, in comparison to the data obtained in cardiomyocytes, no clear effects on the current amplitude were observed. Our results indicate that *Bg*II is about 20 times more potent than *Bg*III. The concentrations for which the half maximal effect on the inactivation process are observed ($EC_{50}$) are 0.38 and 7.8 $\mu$M for *Bg*II and *Bg*III, respectively. In comparison, the $EC_{50}$ of ATX II on cloned hH1 channels expressed in mammalian cells is 11 nM (Chahine *et al*., 1996). *Bg*II, and even more *Bg*III, thus appear to be less powerful inhibitors of the $Na^+$ channel inactivation process than ATX II. Nevertheless, this conclusion has to be considered, at least in part, by the fact that the pharmacological characteristics of the heterologous expression system used (i.e. mammalian cells *vs Xenopus* oocytes) may be different.

The difference in efficiency between *Bg*II and *Bg*III could be surprising regarding the almost identical amino acid sequences of these two toxins. However, our findings are consistent with the results of a previous study by Loret *et al*. (1994) who have shown that the toxicity of *Bg*II injected intracerebroventricularly in mice is more than 50 times superior than the toxicity of *Bg*III. In the same study, the higher toxicity of *Bg*II is correlated with a higher competition binding with the scorpion $\alpha$-toxin AaH II to rat brain synaptosomes. All together, these data strongly suggest that the asparagine in position 16, which is a very conservative residue among type 1 toxins, is an important residue for the toxicity of these toxins.

In parallel to the action on the inactivation process of $Na^+$ currents, our study also reveals that *Bg*II and *Bg*III induce several other modifications of the electrophysiological properties of hH1 channels. Firstly, the steady-state activation and inactivation parameters are shifted to more positive values by the toxins. In comparison, the steady-state activation of hH1 expressed in mammalian cells is not affected by ATX II while the steady-state inactivation is shifted to a more positive potential by about 3 mV (Chahine *et al*., 1996).

The most intriguing observation, in the presence of both toxins, is the shift of the reversal potential of $Na^+$ current generated by hH1. The measured shifts correspond to a 7

fold decrease of the ionic selectivity for $Na^+$ over $K^+$. In comparison, in myocytes, no modifications of the $E_{rev}$ are observed upon addition of *Bg*II and *Bg*III. In control conditions and in the presence of toxins, $E_{rev}$ remains $\sim -10$ mV. In these experiments, the internal concentration of $Na^+$ is higher than the external one (7 mM and 5 mM, respectively) and there is no $K^+$ in solution since it has been replaced by $TEA^+$ and $Cs^+$. One explanation could be that the $E_{rev}$ in the presence of the toxin is not shifted, because, even if the selectivity of the channel is modified, $K^+$ is not present and, except $Na^+$, no other monovalent cations are able to pass through the channel. The $EC_{50}$ values for the observed changes in $E_{rev}$ are 0.34 and 8.4 $\mu$M for *Bg*II and *Bg*III respectively. Here again the potency of *Bg*II is higher than the potency of *Bg*III, confirming the importance of the asparagine in position 16 for the binding and the toxicity of these toxins. Interestingly, the efficacy of *Bg*II and *Bg*III on the change in reversal potential is very similar (a shift of approximately $-16$ mV in both cases), suggesting that the mechanism by which *Bg*II and *Bg*III affect the ionic selectivity of hH1 is different from the one affecting the inactivation time course or steady-state activation. To the best of our knowledge, the modification of the ionic selectivity of $Na^+$ channel has never been observed with any other sea anemone toxins. Nonetheless, several other toxins have been reported to affect the ionic selectivity of $Na^+$ channels. For example, two alcaloid toxins (batrachotoxin isolated from the skin of the Colombian arrow poison frog of the genera *Dendrobates* and *Phyllobates*, as well as aconitine from the plant *Aconitinum napellus*) are able to decrease the ionic selectivity of $Na^+$ channels (Denac *et al*., 2000; Hille, 1992). It is thought that these toxins act by a widening of the selectivity filter. The receptor site of these lipid-soluble toxins is localized within the plasma membrane (receptor site 2) while *Bg*II and *Bg*III bind to a site localized in the extracellular loop between segments S3 and S4, in the fourth domain (D4) (receptor site 3) (Loret *et al*., 1994). It should be mentioned that another toxin which binds to site 3, the $\alpha$-toxin AaH II from the scorpion *Androctonus australis* Hector, has also been reported to modify the reversal potential of $Na^+$ currents (Benoit & Dubois, 1987). On the one hand, it remains difficult to explain how toxin binding to an external site not localized within the pore could decrease the ionic selectivity of the channel. On the other hand, given the negatively charged residues in the outer mouth of rat sodium channels controlling the ion flux and selectivity (Chiamvimonvat *et al*., 1996), it could be hypothesized that the apparent decrease in ionic selectivity of the channel could result from a modification of the surface charges of the external part of the channel due to the binding of the toxin. In this view, the toxin can be considered as a pre-filter interfering with the access of ions to the pore.

In the present study, we have characterized and compared the mode of action of two toxins isolated from the sea anemone *Bunodosoma granulifera*, *Bg*II and *Bg*III, on action potentials of rat ventricular strips, on $Na^+$ currents in rat cardiomyocytes and on the cloned cardiac $Na^+$ channel hH1 expressed in *Xenopus* oocytes. This work is the first electrophysiological characterization of these toxins and reveals that *Bg*II and *Bg*III interact with $Na^+$ channels in cardiac cells, pointing out that these toxins, generally known as neurotoxins, are also cardiotoxic. From a mechanical point of view, our work discloses that, beside the 'classical' effects of sea anemone $Na^+$ channels toxins (slowing of inactivation kinetics, shift of steady-state activation and inactivation parameters), *Bg*II and *Bg*III also induce a decrease of the ionic selectivity of $Na^+$ channels.

We are grateful to Evelyne Dubois and Chris Ulens for fruitful discussions. The hH1 clone was kindly provided by R.G. Kallen. This work was supported by a K.U. Leuven post-doctoral fellowship to C. Goudet and a grant Z-005 from Consejo Nacional de Ciencia y Tecnologia (CONACyT), Mexican Government to L.D. Possani.

## References

ALSEN, C., HARRIS, J.B. & TESSERAUX, I. (1981). Mechanical and electrophysiological effects of sea anemone (*Anemonia sulcata*) toxins on rat innervated and denervated skeletal muscle. *Br. J. Pharmacol.,* **74,** 61–71.

ALVAREZ, J., DORTICO, S.F. & MORLANS, J. (1981). Changes in electrical and mechanical activities of rabbit papillary muscle during hypoxic perfusion. *J. Physiol. (Paris),* **77,** 807–812.

ANEIROS, A., GARCIA, I., MARTINEZ, J.R., HARVEY, A.L., ANDERSON, A.J., MARSHALL, D.L., ENGSTROM, A., HELLMAN, U. & KARLSSON, E. (1993). A potassium channel toxin from the secretion of the sea anemone *Bunodosoma granulifera*. Isolation, amino acid sequence and biological activity. *Biochim. Biophys. Acta.,* **1157,** 86–92.

BALSER, J.R. (1999). Structure and function of the cardiac sodium channels. *Cardiovasc. Res.,* **42,** 327–338.

BENOIT, E. & DUBOIS, J.M. (1987). Properties of maintained sodium current induced by a toxin from *Androctonus* scorpion in frog node of Ranvier. *J. Physiol. (Lond.),* **383,** 93–114.

BENZINGER, G.R., DRUM, C.L., CHEN, L.Q., KALLEN, R.G., HANCK, D.A. & HANCK, D. (1997). Differences in the binding sites of two site-3 sodium channel toxins. *Pflugers Arch.,* **434,** 742–749.

BRUHN, T., SCHALLER, C., SCHULZE, C., SANCHEZ-RODRIGUEZ, J., DANNMEIER, C., RAVENS, U., HEUBACH, J.F., ECKHARDT, K., SCHMIDTMAYER, J., SCHMIDT, H., ANEIROS, A., WACHTER, E. & BERESS, L. (2001). Isolation and characterisation of five neurotoxic and cardiotoxic polypeptides from the sea anemone *Anthopleura elegantissima*. *Toxicon.,* **39,** 693–702.

CATTERALL, W.A. (1995). Structure and function of voltage-gated ion channels. *Annu. Rev. Biochem.,* **64,** 493–531.

CATTERALL, W.A. (2000). From ionic currents to molecular mechanisms: the structure and function of voltage-gated sodium channels. *Neuron.,* **26,** 13–25.

CESTELE, S. & CATTERALL, W.A. (2000). Molecular mechanisms of neurotoxin action on voltage-gated sodium channels. *Biochimie.,* **82,** 883–892.

CHAHINE, M., PLANTE, E. & KALLEN, R.G. (1996). Sea anemone toxin (ATX II) modulation of heart and skeletal muscle sodium channel alpha-subunits expressed in tsA201 cells. *J. Memb. Biol.,* **152,** 39–48.

CHIAMVIMONVAT, N., PEREZ-GARCIA, M.T., TOMASELLI, G.F. & MARBAN, E. (1996). Control of ion flux and selectivity by negatively charged residues in the outer mouth of rat sodium channels. *J. Physiol. (Lond.),* **491,** 51–59.

DASCAL, N. (1987). The use of Xenopus oocytes for the study of ion channels. *CRC Crit. Rev. Biochem.,* **22,** 317–387.

DENAC, H., MEVISSEN, M. & SCHOLTYSIK, G. (2000). Structure, function and pharmacology of voltage-gated sodium channels. *Naunyn Schmiedebergs Arch. Pharmacol.,* **362,** 453–479.

DONGRE, A.R., ENG, J.K. & YATES, J.R., 3RD (1997). Emerging tandem-mass-spectrometry techniques for the rapid identification of proteins. *Trends Biotechnol.,* **15,** 418–425.

GALAN, L., TALAVERA, K., VASSORT, G. & ALVAREZ, J.L. (1998). Characteristics of $Ca^{2+}$ channel blockade by oxodipine and elgodipine in rat cardiomyocytes. *Eur. J. Pharmacol.,* **357,** 93–105.

GELLENS, M.E., GEORGE, JR A.L., CHEN, L.Q., CHAHINE, M., HORN, R., BARCHI, R.L. & KALLEN, R.G. (1992). Primary structure and functional expression of the human cardiac tetrodotoxin-insensitive voltage-dependent sodium channel. *Proc. Natl. Acad. Sci. U.S.A.,* **89,** 554–558.

GOLDIN, A.L., BARCHI, R.L., CALDWELL, J.H., HOFMANN, F., HOWE, J.R., HUNTER, J.C., KALLEN, R.G., MANDEL, G., MEISLER, M.H., NETTER, Y.B., NODA, M., TAMKUN, M.M., WAXMAN, S.G., WOOD, J.N. & CATTERALL, W.A. (2000). Nomenclature of voltage-gated sodium channels. *Neuron,* **28,** 365–368.

GORDON, D., SAVARIN, P., GUREVITZ, M. & ZINN-JUSTIN, S. (1998). Functional anatomy of scorpion toxins affecting sodium channels. *J. Toxicol-Toxin Rev.,* **17,** 131–159.

HAMILL, O.P., MARTY, A., NEHER, E., SAKMANN, B. & SIGWORTH, F.J. (1981). Improved patch-clamp techniques for high-resolution current recording from cells and cell-free membrane patches. *Pflugers Arch.,* **391,** 85–100.

HILLE, B. (1992). Ionic channels of excitable membranes: Sinauer Associates Inc., Sunderland, Massachusetts, USA.

KEM, W.R., PARTEN, B., PENNINGTON, M.W., PRICE, D.A. & DUNN, B.M. (1989). Isolation, characterization, and amino acid sequence of a polypeptide neurotoxin occurring in the sea anemone *Stichodactyla helianthus*. *Biochemistry,* **28,** 3483–3489.

KUDO, Y. & SHIBATA, S. (1980). The potent excitatory effect of a novel polypeptide, anthopleurin-B, isolated from a sea anemone (*Anthopleura xanthogrammica*) on the frog spinal cord. *J. Pharmacol. Exp. Ther.,* **214,** 443–448.

LAZDUNSKI, M., FRELIN, C., BARHANIN, J., LOMBET, A., MEIRI, H., PAURON, D., ROMEY, G., SCHMID, A., SCHWEITZ, H., VIGNE, P. & VIJVERBERG, H.P.M. (1986). Polypeptide toxins as tools to study voltage-sensitive $Na^+$ channels. *Ann. N. Y. Acad. Sci.,* **479,** 204–220.

LIMAN, E.R., TYTGAT, J. & HESS, P. (1992). Subunit stoichiometry of a mammalian K+ channel determined by construction of multimeric cDNAs. *Neuron,* **9,** 861–871.

LORET, E.P., DEL VALLE, R.M., MANSUELLE, P., SAMPIERI, F. & ROCHAT, H. (1994). Positively charged amino acid residues located similarly in sea anemone and scorpion toxins. *J. Biol. Chem.,* **269,** 16785–16788.

MÉNEZ, A. (1998). Functional architectures of animal toxins: a clue to drug design? *Toxicon,* **36,** 1557–1572.

NICHOLSON, G.M., WALSH, R., LITTLE, M.J. & TYLER, M.I. (1998). Characterisation of the effects of robustoxin, the lethal neurotoxin from the Sydney funnel-web spider *Atrax robustus*, on sodium channel activation and inactivation. *Pflügers. Arch.,* **436,** 117–126.

NICHOLSON, G.M., WILLOW, M., HOWDEN, M.E. & NARAHASHI, T. (1994). Modification of sodium channel gating and kinetics by versutoxin from the Australian funnel-web spider *Hadronyche versuta*. *Pflügers. Arch.,* **428,** 400–409.

NORTON, R.S. (1991). Structure and structure-function relationships of sea anemone proteins that interact with the sodium channel. *Toxicon,* **29,** 1051–1084.

NORTON, R.S. (1998). Structure and function of peptide and protein toxins from marine organisms. *J. Toxicol-Toxin Rev.,* **17,** 99–130.

NORTON, T.R. (1981). Cardiotonic polypeptides from *Anthopleura xanthogrammica* (Brandt) and *A. elegantissima* (Brandt). *Fed. Proc.,* **40,** 21–25.

POSSANI, L.D., BECERRIL, B., DELEPIERRE, M. & TYTGAT, J. (1999). Scorpion toxins specific for $Na^+$-channels. *Eur. J. Biochem.,* **264,** 287–300.

RAVENS, U. (1976). Electromechanical studies of an *Anemonia sulcata* toxin in mammalian cardiac muscle. *Naunyn Schmiedebergs Arch. Pharmacol.,* **296,** 73–78.

REIMER, N.S., YASUNOBU, C.L., YASUNOBU, K.T. & NORTON, T.R. (1985). Amino acid sequence of the *Anthopleura xanthogrammica* heart stimulant, anthopleurin-B. *J. Biol. Chem.,* **260,** 8690–8693.

RENAUD, J.F., FOSSET, M., SCHWEITZ, H. & LAZDUNSKI, M. (1986). The interaction of polypeptide neurotoxins with tetrodotoxin-resistant $Na^+$ channels in mammalian cardiac cells. Correlation with inotropic and arrhythmic effects. *Eur. J. Pharmacol.,* **120,** 161–170.

ROGERS, J.C., QU, Y., TANADA, T.N., SCHEUER, T. & CATTERALL, W.A. (1996). Molecular determinants of high affinity binding of alpha-scorpion toxin and sea anemone toxin in the S3-S4 extracellular loop in domain IV of the $Na^+$ channel alpha subunit. *J. Biol. Chem.,* **271,** 15950–15962.

SALINAS, E.M., CEBADA, J., VALDES, A., GARATEIX, A., ANEIROS, A. & ALVAREZ, J.L. (1997). Effects of a toxin from the mucus of the Caribbean sea anemone (*Bunodosoma granulifera*) on the ionic currents of single ventricular mammalian cardiomyocytes. *Toxicon,* **35,** 1699–1709.

SCHWEITZ, H., VINCENT, J.P., BARHANIN, J., FRELIN, C., LINDEN, G., HUGUES, M. & LAZDUNSKI, M. (1981). Purification and pharmacological properties of eight sea anemone toxins from *Anemonia sulcata, Anthopleura xanthogrammica, Stoichactis giganteus*, and *Actinodendron plumosum*. *Biochemistry,* **20,** 5245–5252.

SHIBATA, S., NORTON, T.R., IZUMI, T., MATSUO, T. & KATSUKI, S. (1976). A polypeptide (AP-A) from sea anemone (*Anthopleura xanthogrammica*) with potent positive inotropic action. *J. Pharmacol. Exp. Ther.,* **199,** 298–309.

TANAKA, M., HAINU, M., YASUNOBU, K.T. & NORTON, T.R. (1977). Amino acid sequence of the *Anthopleura xanthogrammica* heart stimulant, anthopleurin A. *Biochemistry,* **16,** 204–208.

ULBRICHT, W. & SCHMIDTMAYER, J. (1981). Modification of sodium channels in myelinated nerve by *Anemonia sulcata* toxin II. *J. Physiol. (Paris),* **77,** 1103–1111.

WILCOX, G.R., FOGH, R.H. & NORTON, R.S. (1993). Refined structure in solution of the sea anemone neurotoxin ShI. *J. Biol. Chem.,* **268,** 24707–24719.

WUNDERER, G. & EULITZ, M. (1978). Amino-acid sequence of toxin I from *Anemonia sulcata*. *Eur. J. Biochem.,* **89,** 11–17.

WUNDERER, G., FRITZ, H., WACHTER, E. & MACHLEIDT, W. (1976). Amino-acid sequence of a coelenterate toxin: toxin II from *Anemonia sulcata*. *Eur. J. Biochem.,* **68,** 193–198.

*(Received April 25, 2001*
*Revised July 20, 2001*
*Accepted September 3, 2001)*